Analog SiPM in planar CMOS technology

Federica Villa, Michele Vergani, Yu Zou, Danilo Bronzi, Alessandro Ruggeri, Franco Zappa
Dipartimento di Elettronica, Informazione e Bioingegneria,
Politecnico di Milano, Piazza Leonardo da Vinci 32, 20133 Milano, Italy
federica.villa@polimi.it

***Abstract*—Silicon Photomultipliers (SiPMs) are emerging single photon detectors used in many applications requiring large active area, photon number resolving capability and immunity to magnetic fields. We developed planar analog SiPMs in a reliable and cost-effective CMOS technology with a total photosensitive area of about 1x1 mm^2. Three devices with different active areas, and fill-factor (21%, 58.3%, 73.7%), have been characterized. The maximum photon detection efficiency is in the near-UV and tops at 38% (including fill-factor), with a dark count rate of 125 kcps. Gain and crosstalk depend on the active area size and are comparable to commercial SiPM. The advantage of a CMOS technology is the possibility to integrate transistors together with the detectors.**

Keywords—Silicon Photomultiplier (SiPM); photon number resolving detector; Positron Emission Tomogaphy (PET); large active area; CMOS technology.

I. INTRODUCTION

Analog Silicon Photomultipliers (SiPM) are large area photodetectors consisting in an array of Single-Photon Avalanche Diodes (SPADs) with passive quenching resistors connected in parallel, usually called "microcells". Differently from digital SiPMs [1], the output is an analog current pulse, proportional to the number of firing microcells. Some properties of SiPMs make them extremely useful devices for many applications, and in particular in single photon detection, in photon number resolved and multi-photons applications.

High Photon Detection Efficiency (PDE) combined with large collection area makes them optimal sensors for single photon detection in applications like Cherenkov imaging [2] and in Near Infra-Red Spectroscopy (NIRS) [3]. Very large area SPADs have been presented in literature [4], and, in principle, they could be used in this kind of applications, but they have a number of disadvantages. In fact SPADs with active area diameter larger than 200 μm typically show high stray capacitances that negatively impact on timing performance and afterpulsing probability, and very high Dark Count Rate (DCR) that almost saturates the device. In SiPMs each cell includes small diameter SPADs, with low stray capacitance and thus low timing jitter and afterpulsing probability, and hot-cells contribute at the output with a sort of constant offset, without saturating the device.

The possibility to have an analog output signal, proportional to the number of simultaneous firing microcells, allows to discriminate how many photons impinge simultaneously on the sensor. This fact makes the SiPM useful in photon number resolved applications, where the number of impinging photons must be measured with single photon resolution in low light conditions, and in multi-photon applications, where the number of absorbed photons must be measured with tens or hundreds counts precision with intense illumination. Examples of photon number resolved applications are the characterization of single-photon sources [4] and quantum information processing [6]. SiPMs are also valid substitutes of Photon-Multipliers Tubes (PMTs) in multi-photon applications, such as Positron Emission Tomography (PET) [7], high energy beam dosimetry [8] and proton therapy [9], because they are insensitive to magnetic fields.

Most commercial analog SiPMs are developed in vertical custom technologies, with p-on-n or n-on-p structure, depending on the spectral range for which they are optimize. Since electrons have an avalanche triggering probability higher than that of holes, p-on-n structures have high PDE in the near-UV range (photon absorption is very superficial), whereas n-on-p structures present higher PDE in the near-IR (photon absorption is more in depth). The exploitation of a custom technology gives the opportunity to tailor dopant concentrations and diffusions width for optimizing SiPM performance, and also to integrate "smart" quenching resistor, in order to improve the fill-factor (FF) [10]-[12]. On the other hand, with custom technologies it is not possible to integrate active components (i.e. transistors) on the same chip.

We developed an analog SiPM in a standard CMOS technology, with high performance in terms of PDE and DCR, with FF comparable to commercial devices. The employment of a standard CMOS technology will enable, for instance, to integrate in each microcell simple electronics to switch-off the most noisy SPADs. In this paper, we present the structure of the three developed SiPMs, with different FF (Section II) and the first characterization of these devices (Section III). Section IV concludes the paper with a comparison between the developed SiPM and some commercial ones.

II. STRUCTURE OF THE CMOS ANALOG SIPM

The developed SiPMs are constituted by 16x16 SPAD cells arranged in 4 macro-pixels (8x8 SPAD cells each) with separate anodes, as shown in Fig. 1. The anode terminal does not correspond exactly to the SPAD anode, because separate quenching resistors have been integrated. The total active area is 928 x 928 μm^2, with 58 μm pitch between adjacent cells.

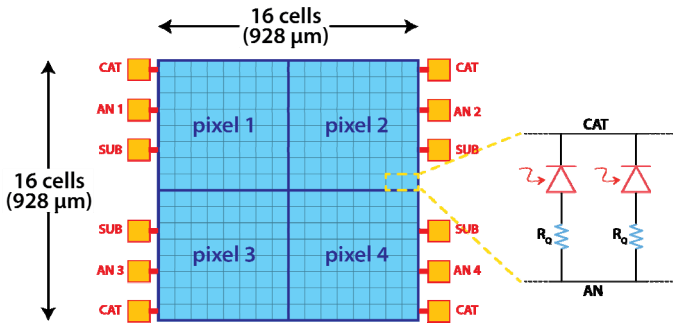

Fig. 1. Left: Structure of the SiPM with 16x16 cells (i.e. 256 SPADs) divided into 4 pixels. Right: Structure of the SPAD cells.

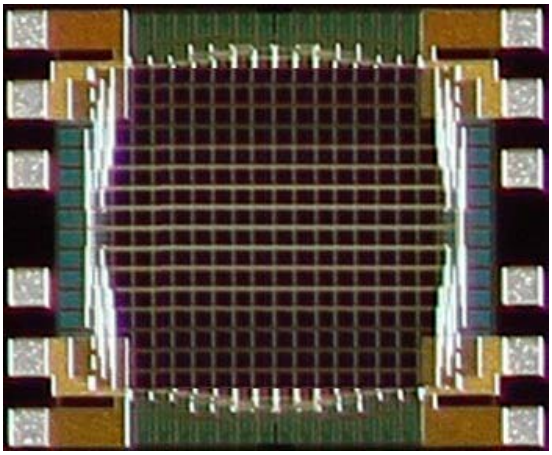

Fig. 2. Micrograph of the S50q SiPM.

Three SiPM families have been developed, with SPADs of different sizes: S30 (30 µm round SPADs, FF = 21.0%), S50 (50 µm round SPADs, FF = 58.3%) and S50q (50 µm square SPADs with rounded corners of 5 µm radius, FF = 73.7%).

Fig. 2 shows a micrograph of the S50q SiPM. The poly-silicon quenching resistances (260 kΩ) have been integrated outside the active area of the SiPM, along the four side of the array, in order to achieve a high FF, with the drawback of limiting the scalability of the device. A unique n-well forms the common cathode of all the SPADs, as shown in the cross-section of the device (Fig. 3).

I. Characterization of the Analog SiPM

The developed SiPMs have been thoroughly characterized, in order to measure the most important parameters for many applications: gain, photoelectron spectrum, PDE, DCR and crosstalk probability. The SiPM readout circuit used in the measurements is based on a transimpedance amplifier, connected to the cathode terminal as shown in Fig. 3. The anodes and the cathodes of the four pixels have been connected in order to obtain an equivalent SiPM with 16 x 16 cells. The feedback resistance (R_f = 2.2 kΩ) determines the gain of the amplifier, whereas the feedback capacitance (C_f = 2.5 pF) has been added to compensate the stage (note that the total capacitance at the cathode terminal is tens of pF).

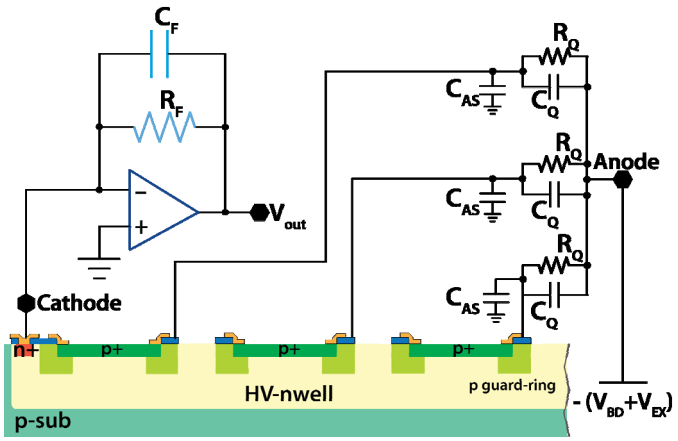

Fig. 3. Cross-section of the standard CMOS SiPM with its readout circuit.

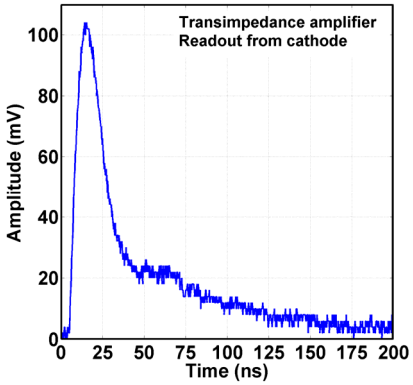

Fig. 4. Output voltage corresponding to a single avalanche of the S30 SiPM. Similar waveforms are obtained with S50 and S50q SiPMs.

The measured breakdown voltage (V_{BD}) is about 25 V with 30 mV/°C temperature coefficient and we operated it typically with excess bias voltage (V_{EX}) between 4 V and 6 V.

The output voltage obtained from a single avalanche (one firing microcell) is shown in Fig. 4. The peak amplitude is 105 mV; the rising edge is exponential with a time constant determined by the internal resistance of the SPAD and the stray anode capacitance (C_{AS}), and it is equal to about 6 ns. When the output reaches the maximum value, the SPAD is quenched and the falling edge is determined by the discharge of the internal SPAD-anode node (C_{AS}, note that it is different from the SiPM-anode terminal), during the reset period. Two time constants are distinguishable: the faster one is due to the presence of a stray capacitance (C_Q) in parallel to the quenching resistance (R_Q) that allows to bypass the resistance itself, whereas the slower one is determined by R_Q and the anode stray capacitances.

A. Gain and photoelectron spectrum

With the term *gain* SiPM users mean the intrinsic charge gain of the SiPM single microcell. The gain is computed with the following formula:

$$G = \frac{V_{EX} \cdot C_{tot}}{q} = \frac{V_{EX} \cdot (C_{ac} + C_{as} + C_q)}{q} \quad (1)$$

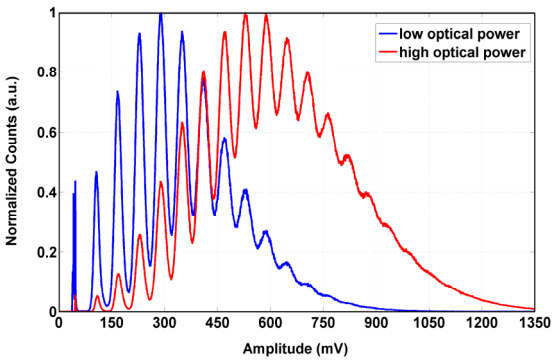

Fig. 5. Photoelectron spectrum of a S50q SiPM.

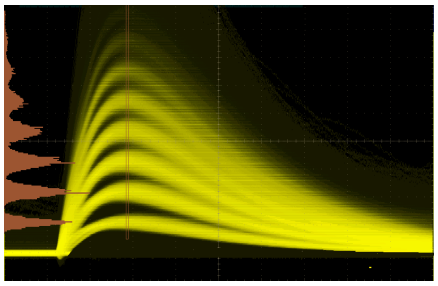

Fig. 6. Output voltage corresponding to multi-photon absorptions.

where C_{ac} is the capacitance between cathode and anode, C_{as} is between anode and substrate, C_q is the capacitance in parallel to the quenching resistor and q is the electron charge. All the parameters have to be referred to one single microcell of the SiPM.

According to Eq. (1), the three developed SiPMs have gains respectively of $8.8 \cdot 10^6$ (S30), $13.2 \cdot 10^6$ (S50), $15.0 \cdot 10^6$ (S50q) at V_{EX} = 5 V. These gains are slightly higher than commercial SiPMs (which are typically $1 \cdot 10^5$ - $5 \cdot 10^6$). Gain together with photoelectron spectrum are important parameters in photon number resolving applications. The photoelectron spectrum has been measured using a multichannel analyzer and illuminating the SiPM with a pulsed laser at 650 nm. The result for a S50q SiPM is shown in Fig. 5, with two different optical powers. Up to 15 simultaneous photon absorptions can be clearly distinguished with single photon precision and the result is confirmed also by the waveform acquired with an oscilloscope (Fig. 6) in low light condition.

B. *Photon Detection Efficiency*

Photon Detection Efficiency (PDE) is the ratio between the number of avalanche pulses and the number of photons that reached the active area. PDE depends on two main processes involved in single-photon detection (i.e. photon absorption efficiency and avalanche multiplication) [13] and on geometrical parameters (fill-factor).

The PDE of a single SPAD developed in the same CMOS technology has been measured at 5 V excess bias and then, multiplying the SPAD PDE by SiPM fill-factor, the PDE spectrum in Fig. 7 has been obtained for S30, S50 and S50q. The peak PDE values (10%, 18%, 38%) are similar to some commercial SiPMs (e.g. from Hamamatsu [14], SensL [15] and AdvanSid [16]), and a bit lower than others (like Ketek ones

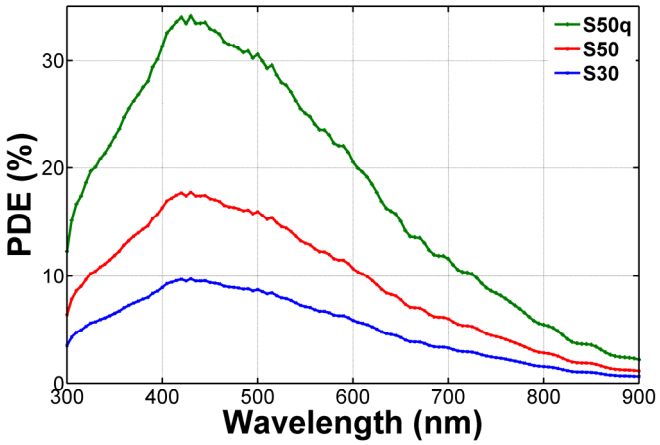

Fig. 7. PDE *vs*. wavelength of the three developed SiPM, including also fill-factor.

that have 50% at 420 nm [17]). The PDE is higher in the near-UV region because the SiPM cross-section is more similar to custom p-on-n than n-on-p structures.

C. *Dark Count Rate*

The Dark Count Rate (DCR) of a SiPM includes the noise contribution of all the microcells, hot-pixels comprised. Therefore the SiPM DCR cannot be computed simply multiplying the typical DCR of a SPAD developed in the same technology by the number of microcells. We measured the DCR connecting the output of the transimpedance amplifier to a counter with 50 mV threshold voltage. At V_{EX} = 5 V the measured DCR of the entire SiPM (16x16 microcells) is 5 kcps, 83 kcps and 125 kcps respectively for S30, S50 and S50q. Fig. 8 shows the detector noise counts at different discriminator thresholds, which correspond to at least one photon absorbed (i.e. 50 mV), two photons absorbed (150 mV) and so on. For the SiPM with higher fill-factor the noise counts contribution is completely negligible with threshold higher than 10 photons.

For a fair comparison between the developed SiPM and the commercially-available ones in terms of dark counts, the DCR has been normalized by the total active area (thus calculating the DCR density). Fig. 9 shows that Hamamatsu ones exploit the cleanest technology and that our SiPM, though developed in planar standard CMOS technology, present DCR density comparable to the others.

D. *Crosstalk probability*

Since a SiPM is composed by many microcells with high fill-factor, crosstalk could be an issue.

We computed the crosstalk probability of our devices with the following formula:

$$Xtalk = \frac{DCR_{2p}}{DCR_{1p}} \tag{3}$$

where DCR_{2p} and DCR_{1p} are the DCRs measured setting the discriminator threshold respectively at two photons and at one

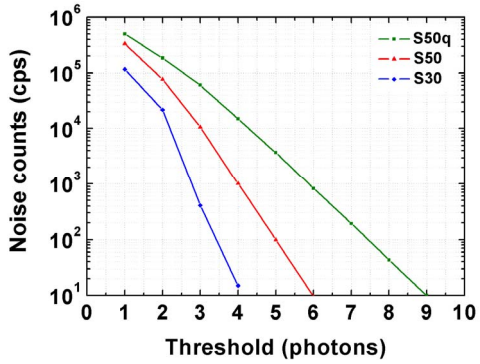

Fig. 8. Noise counts as a function of simultaneous firing microcells.

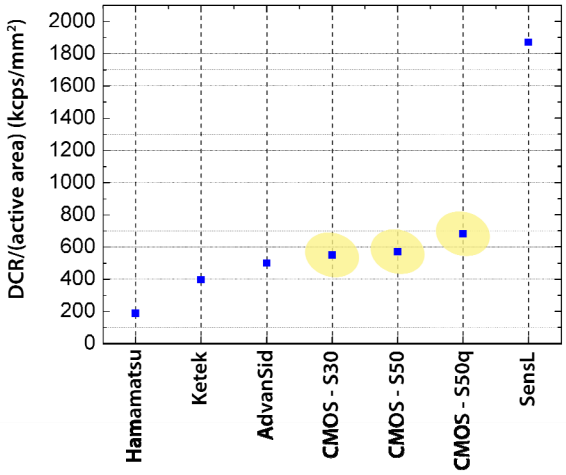

Fig. 9. DCR density comparison between commercial custom SiPMs ([14]-[17]) and our CMOS SiPM.

photon. For the three devices, we obtained 18.6 %, 23.0% and 33.5% respectively for the S30, S50 and S50q SiPMs.These values are comparable to the ones obtained with custom SiPMs without trenches and with the same fill-factor of our SiPMs. SiPMs with trenches instead report lower crosstalk, as low as low 15% with 63% fill-factor (Ketek PM1150 [17]).

II. Discussion and Conclusion

Analog SiPMs in standard planar CMOS technology have been developed and characterized. TABLE I. summarizes the performance of the developed SiPM.

They present high fill-factor (21%, 58%, 73.3% depending on the active area diameter) and peak PDE comparable to commercially-available SiPM developed in custom vertical technologies. The reported SiPMs are able to resolve up to 15 simultaneous photon absorptions with single photon precision. The DCR density is slightly higher than in the most part of the commercial SiPM, but being designed in CMOS technology, in future release, a transistor able to switch off the hot-pixels could be included in each microcell.

Acknowledgment

The authors thanks Micro Photon Devices (MPD) for the support in the SiPM characterization.

TABLE I. Summary of the Performance of the Developed SiPMs

Parameter	*S30*	*S50*	*S50q*	*Unit*
Photosensitive area		928 x 928		μm^2
Microcell pitch		58		µm
Number of microcells		16 x 16		cells
Fill-factor	21.0	58.0	73.3	%
Breakdown temperature coefficient		30		mV/°C
Gain	$8.8 \cdot 10^6$	$13.2 \cdot 10^6$	$15.0 \cdot 10^6$	a.u.
Peak PDE	10	18	38	%
DCR	5	83	125	kcps
Crosstalk	18.6	23.0	33.5	%

References

[1] T. Frach, G. Prescher, C. Degenhardt, R. de Gruyter, A. Schmitz, and R. Ballizany, "The Digital Silicon Photomultiplier - Principle of Operation and Intrinsic Detector Performance," IEEE Nucl. Science Symp., 2009.

[2] H. Miyamoto, M. Teshima, "SiPM development for the imaging Cherenkov and fluorescence telescopes," *Nuclear Instr. and Methods in Physics Research Section A*, vol. 623, no. 1, pp. 198-200, 2010.

[3] A. Dalla Mora, A. Tosi, F. Zappa, S. Cova, D. Contini, A. Pifferi, et al., "Fast-gated single-photon avalanche diode for wide dynamic range near infrared spectroscopy," *IEEE Journal on Selected Topics in Quantum Electronics*, vol. 16, no.4, pp. 1023-1030, 2010.

[4] F. Villa, D. Bronzi, Y. Zou, C. Scarcella, G. Boso, S. Tisa, A. Tosi, F. Zappa, D. Durini, S. Weyers, W. Brockherde, U. Paschen, "CMOS SPADs with up to 500 µm diameter and 55% detection efficiency at 420 nm," Journal of Modern Optics, Jan. 2014.

[5] M.D. Eisaman, J. Fan, A. Migdall, and S.V. Polyakov, "Single-photon sources and detectors," *Rev. of Scientific Instr.*, vol. 82, 071101, 2011.

[6] R.H. Hadfield, "Single-photon detectors for optical quantum information applications," *Nat Photon*, vol. 3, no.12, pp. 696-705, 2009.

[7] D.J. Herbert, S. Moehrs, N. D'Ascenzo, N. Belcari, A. Del Guerra, et al., "The Silicon Photomultiplier for application to high-resolution Positron Emission Tomography," *Nuclear Instruments and Methods in Physics Research Section A: Accelerators, Spectrometers, Detectors and Associated Equipment*, vol. 573, no. 1-2, pp. 84-87, 2007.

[8] A.S. Beddar, T.R. Mackie, and F.H. Attix, "Water-equivalent plastic scintillation detectors for High-energy beam dosimetry: I. Physical characteristics and theoretical consideration," *Phys. Med. Biol.*, vol. 37, no. 10, pp. 1883–1900, 1992.

[9] I. Perali, A. Celani, P. Busca, C. Fiorini, A. Marone, et al., "Prompt gamma imaging with a slit camera for real-time range control in proton therapy: Experimental validation up to 230 MeV with HICAM and development of a new prototype," *Nuclear Science Symposium and Medical Imaging Conference (NSS/MIC)*, pp. 3883-3886, 2012.

[10] N. D'Ascenzo and V. Saveliev, "The New Photo-Detectors for High EnergyPhysics and Nuclear Medicine", *Photodiodes – Comm., Bio-Sensings, Measurements and High-Energy Physics*, pp. 261-284, 2011.

[11] J. Ninkovic´, L. Andric, G. Liemann, G. Lutz, H.G. Moser, et al., "SiMPl, an avalanche diode array with bulk integrated quench resistors for single photon-detection," *Nuclear Instruments and Methods in Physics Research*, vol. 617, pp. 407–410, 2010.

[12] F. Sun, N. Duan, and G.Q. Lo, "Novel Silicon Photomultiplier With Vertical Bulk-Si Quenching Resistors," *IEEE Electron Device Letters*, vol. 34, 2013.

[13] F. Zappa, S. Tisa, A. Tosi, S. Cova, "Principles and features of single-photon avalanche diode arrays," Sensors and Actuators A-Physical, pp. 103-112, 2007.

[14] Hamamatsu S12571-015: www.hamamatsu.com

[15] SensL Bseries-10035: www.SensL.com

[16] AdvanSiD ASD-RGB1S-P/ASD-NUV1S-P: www.advansid.com

[17] Ketek PM1150: www.ketek.net